Vacuum in quantum optics: Progress on a plan

Ninad R. Jetty

with C. S. Unnikrishnan

FILAB, TIFR

DHEP Meeting 2016

Apr. 08, 2016

Beamsplitter with single input

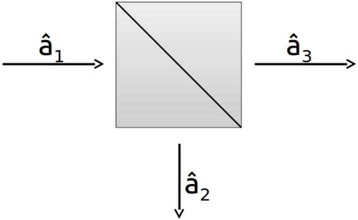

Figure : Input and output fields for a beam splitter.

$$\hat{a}_2 = r\hat{a}_1; \qquad \hat{a}_3 = t\hat{a}_1 \tag{1}$$

Beamsplitter with single input

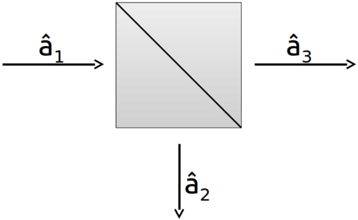

Figure : Input and output fields for a beam splitter.

$$\hat{a}_2 = r\hat{a}_1; \qquad \hat{a}_3 = t\hat{a}_1 \tag{1}$$

$$[\hat{a}_2, \hat{a}_2^\dagger] = |r|^2[\hat{a}_1, \hat{a}_1^\dagger] = |r|^2 \neq 1 \tag{2}$$

$$[\hat{a}_3, \hat{a}_3^\dagger] = |r|^2[\hat{a}_1, \hat{a}_1^\dagger] = |t|^2 \neq 1 \tag{3}$$

$$[\hat{a}_2, \hat{a}_3^\dagger] = rt^* \neq 0 \tag{4}$$

Beamsplitter with two inputs

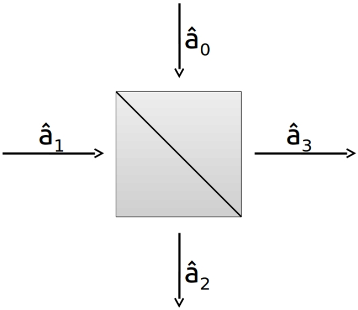

Figure : Two input fields to a beamsplitter.

$$\hat{a}_2 = t'\hat{a}_0 + r\hat{a}_1; \qquad \hat{a}_3 = r'\hat{a}_0 + t\hat{a}_1 \tag{5}$$

Beamsplitter with two inputs

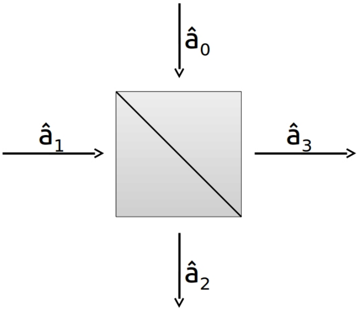

Figure : Two input fields to a beamsplitter.

$$\hat{a}_2 = t'\hat{a}_0 + r\hat{a}_1; \qquad \hat{a}_3 = r'\hat{a}_0 + t\hat{a}_1 \tag{5}$$

$$[\hat{a}_2, \hat{a}_2^\dagger] = |r|^2 + |t'|^2 = 1 \tag{6}$$

$$[\hat{a}_3, \hat{a}_3^\dagger] = |t|^2 + |r'|^2 = 1 \tag{7}$$

$$[\hat{a}_2, \hat{a}_3^\dagger] = rt^* + t'r'^* = 0 \tag{8}$$

Vacuum in Quantum Optics

$$\hat{a}_2 = \sqrt{\frac{1}{2}}[\hat{a}_0 + \iota\hat{a}_1]; \qquad \hat{a}_3 = \sqrt{\frac{1}{2}}[\iota\hat{a}_0 + \hat{a}_1] \tag{9}$$

$$\therefore \hat{a}_1^\dagger = \sqrt{\frac{1}{2}}[\iota\hat{a}_2^\dagger + \hat{a}_3^\dagger] \tag{10}$$

$$|0\rangle_0|1\rangle_1 = \hat{a}_1^\dagger|0\rangle_0|0\rangle_1 \tag{11}$$

Vacuum in Quantum Optics

$$\hat{a}_2 = \sqrt{\frac{1}{2}}[\hat{a}_0 + \iota\hat{a}_1]; \qquad \hat{a}_3 = \sqrt{\frac{1}{2}}[\iota\hat{a}_0 + \hat{a}_1] \tag{9}$$

$$\therefore \hat{a}_1^\dagger = \sqrt{\frac{1}{2}}[\iota\hat{a}_2^\dagger + \hat{a}_3^\dagger] \tag{10}$$

$$|0\rangle_0|1\rangle_1 = \hat{a}_1^\dagger|0\rangle_0|0\rangle_1 \tag{11}$$

- And explain the action of a $50-50$ beam splitter on a single photon.

$$|0\rangle_0|1\rangle_1 \rightarrow \sqrt{\frac{1}{2}}[\iota\hat{a}_2^\dagger + \hat{a}_3^\dagger]|0\rangle_2|0\rangle_3$$
$$= \sqrt{\frac{1}{2}}[\iota|1\rangle_2|0\rangle_3 + |0\rangle_2|1\rangle_3] \tag{12}$$

Problem with Zero Point Energy (ZPE)

- It is in conflict with cosmology:

$$\frac{\dot{a}^2 + kc^2}{a^2} = \frac{8\pi G\rho + \Lambda c^2}{3} \tag{13}$$

Problem with Zero Point Energy (ZPE)

- It is in conflict with cosmology:

$$\frac{\dot{a}^2 + kc^2}{a^2} = \frac{8\pi G\rho + \Lambda c^2}{3} \tag{13}$$

- The (zero point) energy density in the universe is:

$$\rho_0(\omega) = \frac{\hbar\omega^3}{2\pi^2 c^3} \implies \int_{\omega_1}^{\omega_2} d\omega \rho_0(\omega) = \frac{\hbar}{8\pi^2 c^3}(\omega_2^4 - \omega_1^4) \tag{14}$$

Problem with Zero Point Energy (ZPE)

- It is in conflict with cosmology:

$$\frac{\dot{a}^2 + kc^2}{a^2} = \frac{8\pi G\rho + \Lambda c^2}{3} \quad (13)$$

- The (zero point) energy density in the universe is:

$$\rho_0(\omega) = \frac{\hbar\omega^3}{2\pi^2 c^3} \implies \int_{\omega_1}^{\omega_2} d\omega \rho_0(\omega) = \frac{\hbar}{8\pi^2 c^3}(\omega_2^4 - \omega_1^4) \quad (14)$$

- Not only non-negligible, in fact huge ($\sim 10^{-9}$ erg/cm^3):
  - ~ 220 erg/cm^3 in the visible spectrum
  - $\sim 10^{35}$ erg/cm^3 for wavelengths ranging from classical electron radius to size of universe.

Problem with Zero Point Energy (ZPE)

- It is in conflict with cosmology:

$$\frac{\dot{a}^2 + kc^2}{a^2} = \frac{8\pi G\rho + \Lambda c^2}{3} \tag{13}$$

- The (zero point) energy density in the universe is:

$$\rho_0(\omega) = \frac{\hbar\omega^3}{2\pi^2 c^3} \implies \int_{\omega_1}^{\omega_2} d\omega \rho_0(\omega) = \frac{\hbar}{8\pi^2 c^3}(\omega_2^4 - \omega_1^4) \tag{14}$$

- Not only non-negligible, in fact huge ($\sim 10^{-9}$ erg/cm^3):
    - ~ 220 erg/cm^3 in the visible spectrum
    - $\sim 10^{35}$ erg/cm^3 for wavelengths ranging from classical electron radius to size of universe.
- No direct experimental evidence.

Our Proposal

- ZPE is essential for theoretical consistency of all quantum theories.

Our Proposal

- ZPE is essential for theoretical consistency of all quantum theories.
- But only that of matter is physically real, in the form of zero point motion; its existence supported by experiments.

Our Proposal

- ZPE is essential for theoretical consistency of all quantum theories.
- But only that of matter is physically real, in the form of zero point motion; its existence supported by experiments.
- In case of light, one of the following is true:
  - ZPE is not physically real; its effects being manifest due to interaction with matter.

Our Proposal

- ZPE is essential for theoretical consistency of all quantum theories.
- But only that of matter is physically real, in the form of zero point motion; its existence supported by experiments.
- In case of light, one of the following is true:
  - ZPE is not physically real; its effects being manifest due to interaction with matter.
  - It is physically real; i.e. there is no consistent description of the beam splitter without invoking the vacuum energy.

Our Proposal

- ZPE is essential for theoretical consistency of all quantum theories.
- But only that of matter is physically real, in the form of zero point motion; its existence supported by experiments.
- In case of light, one of the following is true:
  - ZPE is not physically real; its effects being manifest due to interaction with matter.
  - It is physically real; i.e. there is no consistent description of the beam splitter without invoking the vacuum energy.
- The aim is to give a consistent description of quantum optical experiments, but without invoking the physical reality of vacuum.

Spontaneous Parametric Downconversion (SPDC)

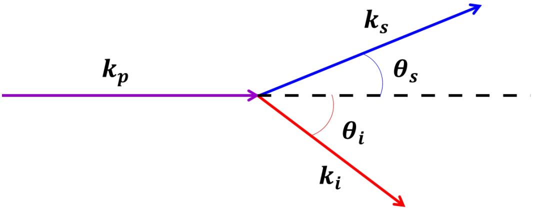

Figure : Schematic of the downconversion process.

$$\mathbf{k_p} = \mathbf{k_s} + \mathbf{k_i} \tag{16}$$

$$n_p k_p = n_s k_s \cos\theta_s + n_i k_i \cos\theta_i \tag{17}$$

$$n_p = n_s \cos\theta_c \tag{18}$$

Types of SPDC

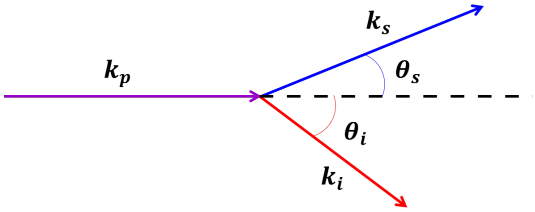

Figure : Schematic of the downconversion process.

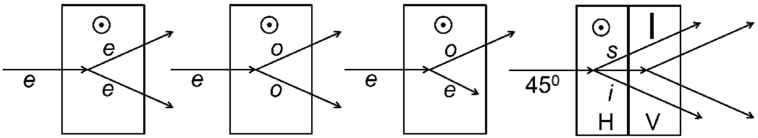

Figure : Type-0, Type-I, Type-IIa, and Type-IIb SPDC processes.

A Source of Entangled Photons

- Deterministic vs Probabilistic Sources

A Source of Entangled Photons

- Deterministic vs Probabilistic Sources

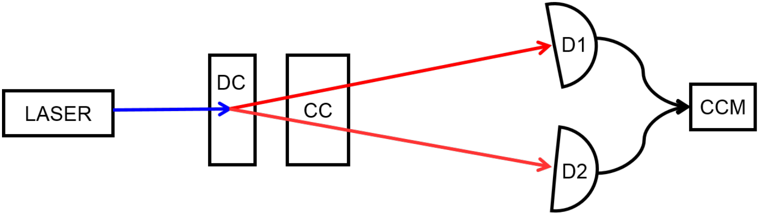

Figure : Schematic of the single photon source.

$$|V\rangle_p \rightarrow |H\rangle_s |H\rangle_i \quad (19)$$

$$|H\rangle_p \rightarrow e^{\iota\Delta} |V\rangle_s |V\rangle_i \quad (20)$$

$$|\psi_p\rangle = \cos\theta_p |V\rangle_p + e^{\iota\phi_p} \sin\theta_p |H\rangle_p \quad (21)$$

$$\therefore |\psi_{DC}\rangle = \cos\theta_p |H\rangle_s |H\rangle_i + e^{\iota\phi} \sin\theta_p |V\rangle_s |V\rangle_i \quad (22)$$

Counts vs input power

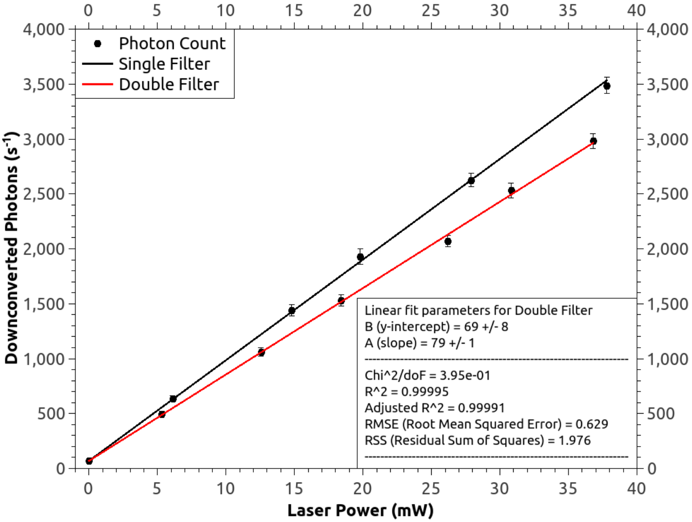

Figure : Downconversion photon number is expected to be proportional to the pump power.

Counts vs input polarization

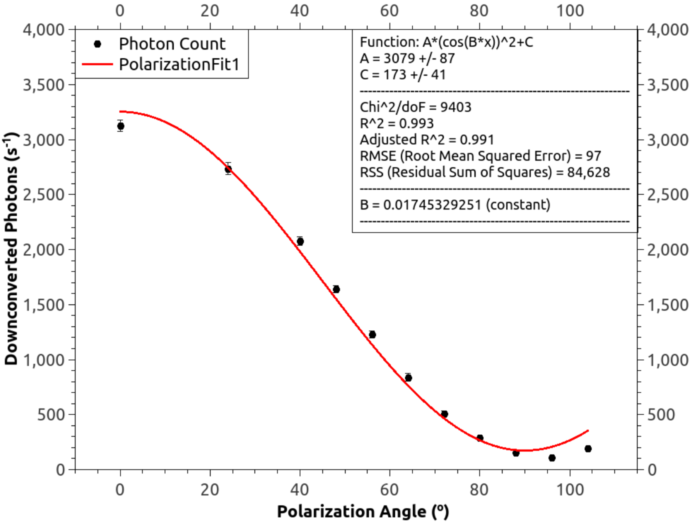

Figure : Downconversion photon number is expected to follow a $\cos^2\theta$ with variation in the polarization angle θ_p.

Angular spread of beam

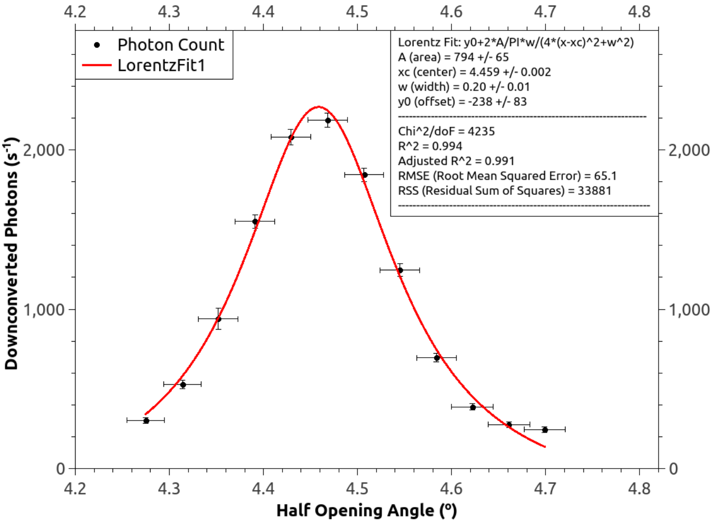

Figure : The angular spread of the downconverted photons is 0.2°.

Quantum Cloning[1]

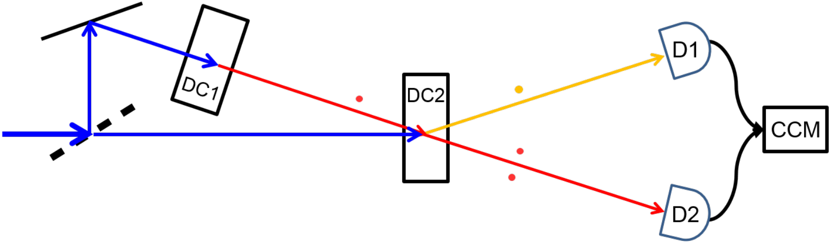

Figure : The input photon stimulates the PDC process thereby allowing for cloning of the input state. The spontaneous emission noise seems to prevent the violation of the no-cloning theorem. This will help explore the role of spontaneous emission and hence that of the quantum vacuum in preventing cloning.

[1] Lamas-Linares, A., Simon, C., Howell, J. C. & Bouwmeester, D. Experimental quantum cloning of single photons. Science 296, 712-4 (2002)

Acknowledgements

- Prof. C. S. Unnikrishnan.
- Prof. Y. V. G. S. Murti, Prof. D. N. Rao, and Prof. C. Vijayan; Dr. N. P. Rajesh and Prof. K. Porsezian.
- Prof. R. P. Singh, Dr. Gautam Samantha, Ali, Nijal, and Jabir
- Prof. G Krishnamoorthy, Dr. Achanta venu Gopal, Dr. Sushil Mujumdar, and Mr. Randhir Kumar.
- Dr. G. Rajalakshmi, Dr. T. R. Saravanan, and Mr. Dipankar Nath.
- Mr. P. V. Sudersanan, Mr. P. G. Rodrigues, and Mr S. K. Guram.
- Friends for interesting discussions and questions.

Some observations

- In Planck's derivation [1912] the average oscillator energy contains a zero point energy (ZPE), not radiation.

$$\rho(\omega) - \frac{\omega}{3}\frac{d\rho}{d\omega} = \left(\frac{\pi^2 c^3}{3\omega^2 k_B T}\right)\rho^2(\omega) \quad \text{...[E-H 1910]} \tag{23}$$

- The solution to Eq. (23) satisfying $\rho(0) = 0$ is the R-J law, derived classically as a result of light-matter interaction.

$$\rho(\omega) - \frac{\omega}{3}\frac{d\rho}{d\omega} = \frac{1}{3k_B T}\rho(\omega)U \tag{24}$$

$$\rho(\omega) - \frac{\omega}{3}\frac{d\rho}{d\omega} = \frac{\pi^2 c^3}{3\omega^2 k_B T}\left[\rho^2(\omega) + \frac{\hbar\omega^3}{\pi^2 c^3}\rho(\omega)\right] \quad \text{...[E-S 1913]} \tag{25}$$

- Einstein and Stern [1913] noted that adding a ZPE (of $\hbar\omega$) to the oscillators in the classical model leads to the Planck spectrum.

Casimir Effect

- The Casimir-Polder calculations[2] use perturbation theory on atomic levels inside a box, and are "not in disagreement" with a classical calculation involving retarded fields.
- Casimir[3], derived the force using difference in vacuum energy.

$$\delta E = \frac{L^2}{\pi^2}\hbar c \left[\sum_n{}' \int_0^\infty \int_0^\infty dk_x dk_y \sqrt{k_x^2 + k_y^2 + \frac{n^2\pi^2}{a^2}} - \frac{a}{\pi} \int_0^\infty \int_0^\infty \int_0^\infty dk_x dk_y dk_z \sqrt{k_x^2 + k_y^2 + k_z^2} \right] \tag{26}$$

- The generalization of Casimir-force by Lifshitz, for real metals and dielectrics using only molecular forces between particles has been tested experimentally.

[2] Casimir, H. B. G. & Polder, D. The Influence of Retardation on the London-van der Waals Forces. Phys. Rev. 73, 360372 (1948).

[3] Casimir, H. On the attraction between two perfectly conducting plates. Proc. K. Ned. Akad. Wet 51, 793795 (1948).

Spontaneous emission

- Einstein's derivation of Planck spectrum.

$$\rho(\omega_0)B_{12}N_1 = \rho(\omega_0)B_{21}N_2 + A_{21}N_2 \tag{27}$$

$$\rho(\omega_0) = \frac{A_{21}N_2}{B_{12}N_1 - B_{21}N_2} = \frac{A_{21}/B_{21}}{\frac{B_{12}}{B_{21}}\frac{N_1}{N_2} - 1} = \frac{A_{21}/B_{21}}{e^{\hbar\omega/k_B T} - 1} \tag{28}$$

$$\frac{A_{21}}{B_{21}} = \frac{\hbar\omega_0^3}{\pi^2 c^3} \quad [\equiv 2\rho_0(\omega_0)] \tag{29}$$

- Not *all* stimulated emission by vacuum.

$$(\dot{N}_2)^0_{stiem} = -B_{21}\rho_0(\omega_0)N_2 \equiv -\frac{1}{2}A_{21}N_2 = \frac{1}{2}(\dot{N}_2)_{spoem} \tag{30}$$

- Identical energy density as that of radiation reaction.

$$(\rho_0)_{eff} = \frac{1}{6}\rho_0(\omega)\Delta\omega = \frac{1}{18\pi}\mu^2\left(\frac{\omega}{c}\right)^6 \tag{31}$$

$$(\rho_0)_{RR} = \frac{E_{RR}^2}{8\pi} = \frac{1}{18\pi}\mu^2\left(\frac{\omega}{c}\right)^6 \tag{32}$$

The SPDC-based SPS

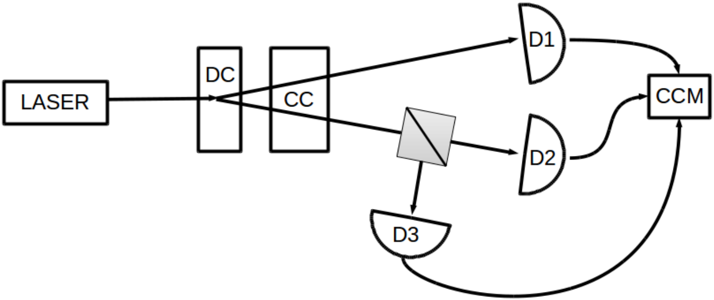

Figure : Proving the existence of photons in our setup.

High-Efficiency Single-Photon Detectors

Figure : The ID120, from ID Quantique, is a Si-APD operating in Geiger Mode; eff. $\sim 80\ \%$ around 810 nm.

Feature	Specification
Wavelength range	350 to 1000 nm
Active area	500 μm^2
Quenching mechanism	Passive
Output pulse width*	30 ns
Deadtime	400 ns
Dark count rate (Hz)*	
at excess bias 10 V, -40^0 C	31
at excess bias 20 V, -40^0 C	52
at excess bias 30 V, -40^0 C	70
at excess bias 40 V, -40^0 C	86
Single-photon detection efficiency	
at 650 nm (at max. excess bias)	55 %
at 800 nm (at max. excess bias)	80 %

Table : Important specifications of the ID120 SPAD.

Dark count characteristics

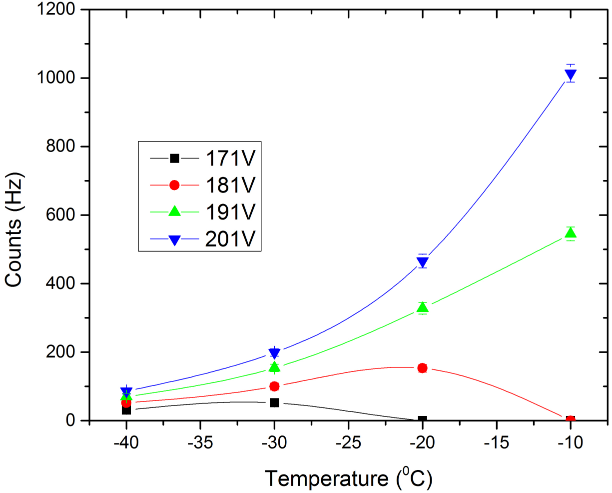

Figure : Dark counts depend on both, temperature as well as bias voltage.

Measured FPGA characteristics

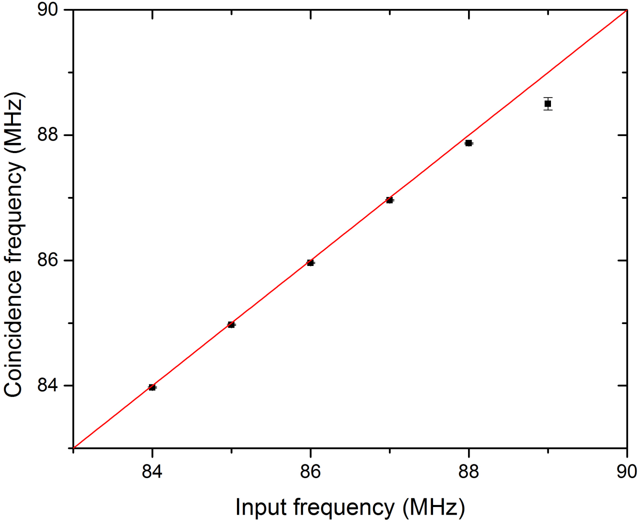

Figure : The result of testing our CCM with regular input pulses.

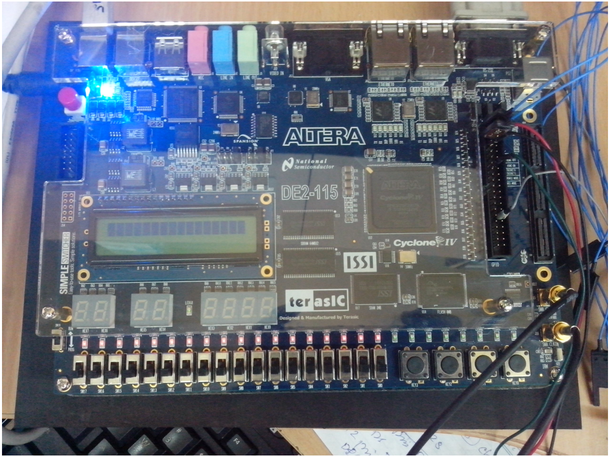

Figure : The DE2-115 FPGA board.

Problem: normal dispersion

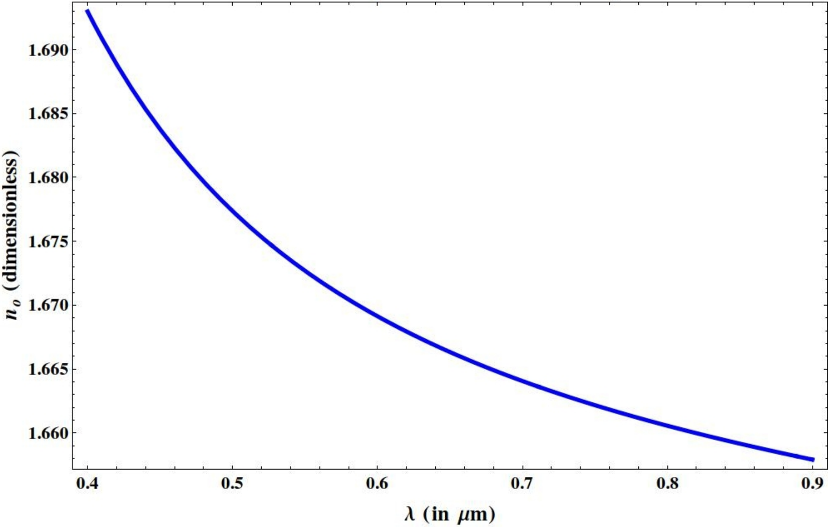

Figure : $n_p > n_s$, where $\lambda_p < \lambda_s$ does not allow Eq. (18) to be satisfied.

Solution: birefringence

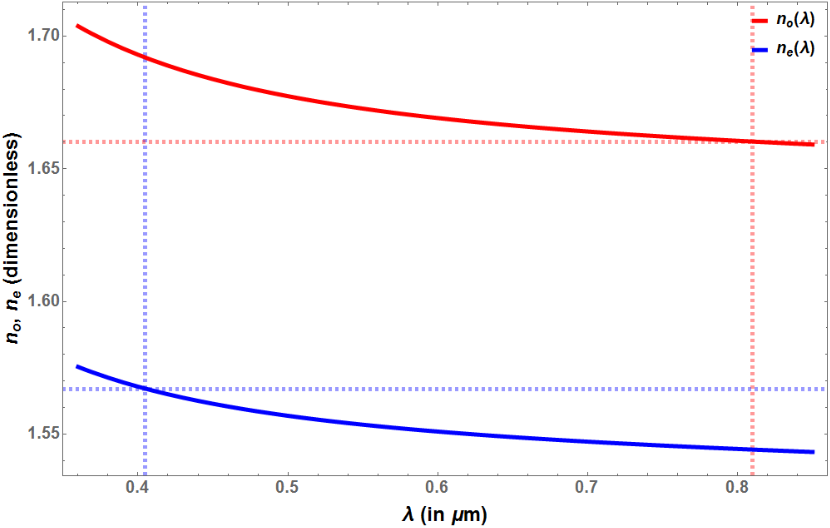

Figure : $n_p^e = n_s^o \cos\psi_c$ can now be be satisfied.

Solution: birefringence

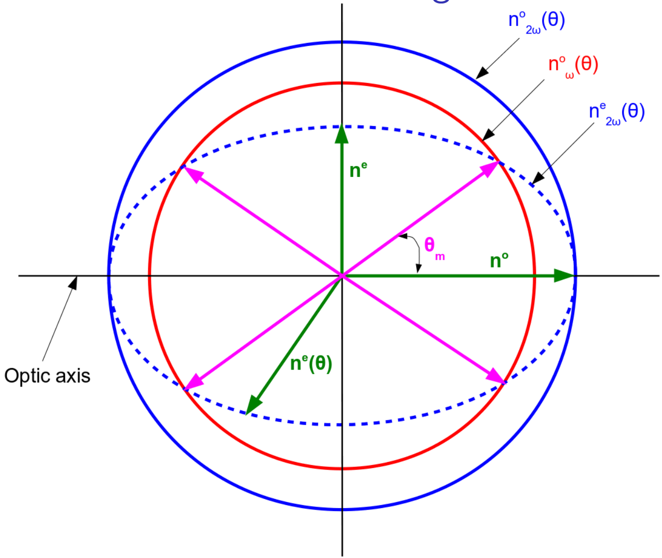

Figure : The refractive index ellipsoids for a negative, uniaxial crystal.

Compensation

- In type-I or type-0 phase-matching, both photons accumulate the same phase.
- In type-II, that is not the case.[5]
- And so it is not, for a pair of type-I or type-0 crystals in crossed-axis arrangement.[6]

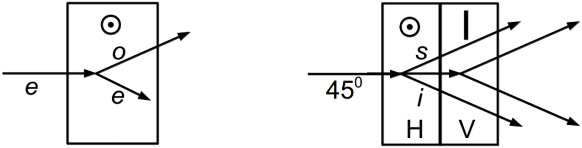

Figure : Type-II proper and type-I crossed axis phase-matching.

[5] Kwiat, P. et al. New High-Intensity Source of Polarization-Entangled Photon Pairs. Phys. Rev. Lett. 75, 43374341 (1995).

[6] Kwiat, P. G., Waks, E., White, A. G., Appelbaum, I. & Eberhard, P. H. Ultrabright source of polarization-entangled photons. Phys. Rev. A 60, R773R776 (1999).

Compensating crossed-axis DCs of Type-0,I

$$\phi_d = 2\pi L \left[\frac{n^e(\lambda_s)}{\lambda_s} + \frac{n^e(\lambda_i)}{\lambda_i} \right] \qquad \text{for} \begin{cases} ooo \\ ooe \end{cases} \tag{42}$$

$$\phi_c = 2\pi L_c \left\{ \left[\frac{n_c^e(\lambda_s)}{\lambda_s} - \frac{n_c^o(\lambda_s)}{\lambda_s} \right] + \left[\frac{n_c^e(\lambda_i)}{\lambda_i} - \frac{n_c^o(\lambda_i)}{\lambda_i} \right] \right\} \tag{43}$$

- The idea is to set $\phi_d + \phi_c = 0$ and solve for L_c, the compensator length.
- Usually, the downconversion and compensator crystals are of opposite variety; a negative compensator is used for a positive downconversion crystal, and vice versa.

Deciding laser specifications

- The pump wavelength is 405 nm. The frequency-bandwidth constrains the allowed beam-divergence.
- For small deviations ($\Delta\theta$) from the phase-matching angle (θ_{pm}), the efficiency decreases[7] as $sinc^2(\Delta kL/2)$

$$\Delta k(\theta - \theta_{pm}) \simeq \left.\frac{\partial(\Delta k)}{\partial\theta}\right|_{\theta=\theta_{pm}} (\Delta\theta) + \frac{1}{2}\left.\frac{\partial^2(\Delta k)}{\partial\theta^2}\right|_{\theta=\theta_{pm}} (\Delta\theta)^2 \quad (51)$$

$$\equiv \gamma_{CPM}\ (\Delta\theta) + \gamma_{NCPM}\ (\Delta\theta)^2 \quad (52)$$

- Since $\Delta k_{BW} L = 2.784$, the angular bandwidth ($\Delta\theta_{BW}$) is related to γ by

$$\Delta\theta_{BW}^{CPM} = \frac{2.784}{\gamma_{CPM} L} \quad (53) \qquad \Delta\theta_{BW}^{NCPM} = \left[\frac{2.784}{\gamma_{NCPM} L}\right]^{\frac{1}{2}} \quad (54)$$

[7] Sutherland, R. L. Handbook of nonlinear optics, Marcel Dekker, Inc. 2e (2003). ISBN: 0-8247-4243-5

Bounding the beam-divergence

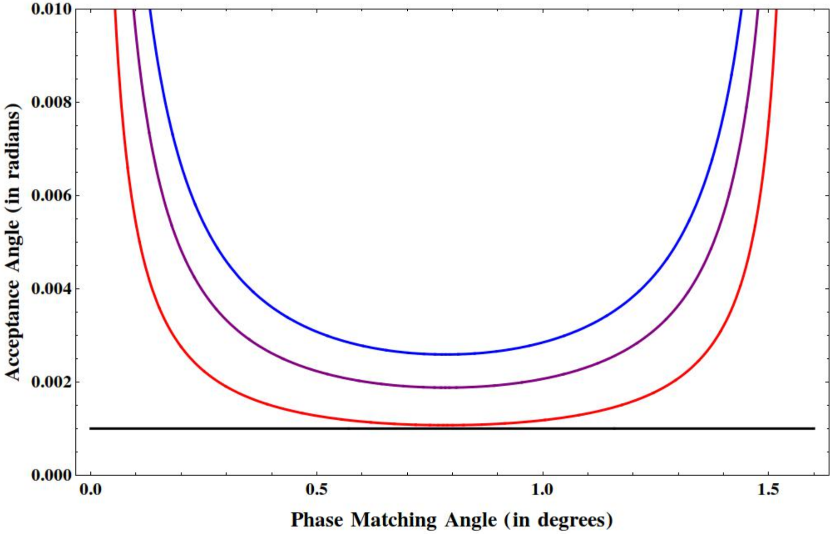

Figure : Plot of acceptance angle over $[0,\pi/2]$, behaviour is same throughout; $L = 3.0$ mm, $\lambda_\omega = 810$ nm.

The ONDAX Laser

Figure : The 405 ± 0.5 nm single mode laser; specifications given below.

Feature	Specification
Coherence Length	~ 1.8 m
Max Output Power	40 mW
Max Beam Divergence	10 mrad
Beam Size	0.8×0.4 mm

Higher order interference

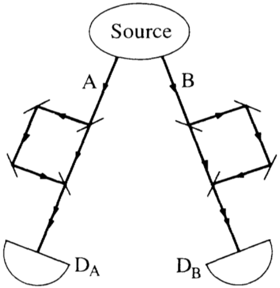

Figure : A proposed higher order interference experiment by Franson.

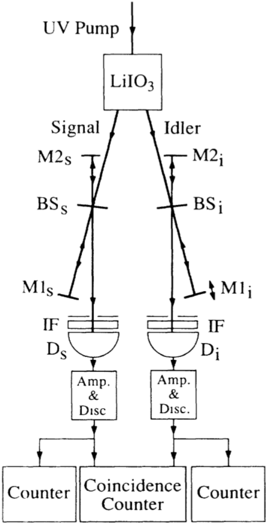

Figure : Experimental setup of Ou *et. al.*[5]

[5] Ou, Z., Zou, X., Wang, L. & Mandel, L. Observation of nonlocal interference in separated photon channels. Phys. Rev. Lett. 65, 321324 (1990).

A Tunable Laser

Figure : The 405 ± 0.5 nm single mode laser; specifications given below.

Feature	Specification
Coherence Length	> 20 m
Max Output Power	$40, 80$ mW
Max Beam Divergence	1 mrad
Beam Size	~ 1 mm

Working with KTP

- KTP is a ferroelectric, biaxial crystal, and it can be quasi phase-matched.
- Crystal is grown with its ferroelectric domains orthogonally oriented after every coherence length $l_c \sim 2\pi/\Delta k$.
- During crystal growth by using large electric fields.
- Relaxes the condition for phase-matching;
- But with large crystals, the accumulated phase is also huge $\sim 3000^\circ$.

Compensated phase-map for ppKTP-YVO

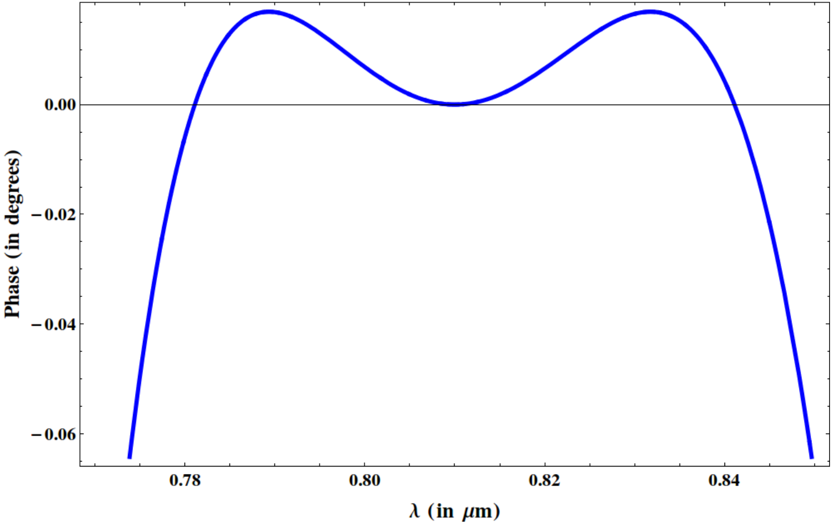

Figure : Length of the compensator is 31.11 mm, for two 20 mm type-0 phase-matched ppKTP crystals in crossed-axis arrangement.

Induced coherence[2]

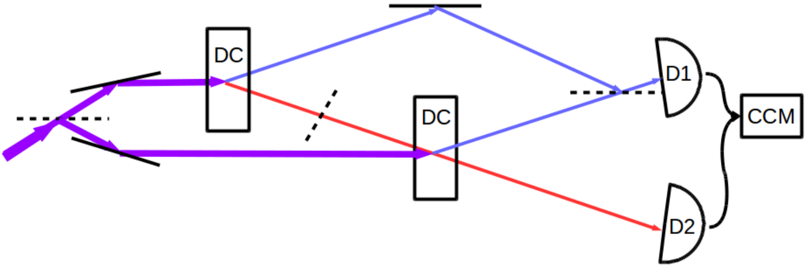

Figure : Schematic of the experimental setup for studying Induced Coherence. The indistinguishability of the idler photons determines the visibility of the fringes formed by the signal photons. We would like to explore if the phase relationship between the idler photons affects the correlations.

[2]Zou, X., Wang, L. & Mandel, L. Induced coherence and indistinguishability in optical interference. Phys. Rev. Lett. 67, 318321 (1991).